Jet-flap installation noise of pylon mounted jet engine on 3D wing

Christian Jente*

German Aerospace Center (DLR), Lilienthalplatz 7, D-38108 Braunschweig, Germany

The purpose of this paper is to investigate the velocity scaling of jet-flap interference noise for a fixed build in static or flight operations. The flap trailing edge is located outside the isolated jet's mixed jet radius and for the experimental data even outside the isolated jet's outer shear layer, i.e. not inside the cone with half-opening angle of 7.5° for static jet operations.

The engine is pylon-mounted, hence the pylon shifts the virtual shear layer origin of the outer jet shear layer near the flap and disrupts its coherence. The experimental data does not show significant mid-frequency broadband noise components and tones while the low-frequency jet installation noise effect is observed.

Hence, this paper contains analytical work to characterize the low-frequency noise: the far-field solution of Ffowcs-Williams Hawking and Curle for the interaction of fixed and rigid bodies with unsteady flow fluctuations is interpreted wrt the jet-flap interference problem. The sound intensity for compact noise is found to scale with $I \propto (\Delta U)^6$. The derived relation is further decomposed into dimensionless terms for the effects of flight operations, temperature behavior and geometry.

There is suitable experimental test data in the Aeroacoustic Windtunnel Braunschweig to invesitigate the flight operations effect. Experimental jet installation noise data is cross-compared in the direction perpendicular to the flap where the low-frequency maximum was detected. The data is scaled for various interesting velocity exponents, i.a. q=5 for trailing edge noise, q=6 for compact noise and q=8 for free turbulence and wrt various velocity candidates.

*Research Engineer, Department of Technical Acoustics, christian.jente@dlr.de

I. Introduction

Nomenclature

Name	Unit	Meaning
α	[-]	shear layer convection coefficient, $\alpha = 0.64$
ΔU	[Hz]	shear layer difference velocity
$\Delta\delta_\omega$	[m]	shear layer width
γ	[-]	adiabatic index
λ	[-]	wave length
ρ_∞	[kg/m^3]	(static) density of medium in acoustic room
ρ_j	[kg/m^3]	static density of jet
$\boldsymbol{\tau}$	[Pa]	viscous stress tensor
θ	[°]	polar angle of microphone, from engine exhaust (aft-front)
A	[m^2]	area
a_j	[m/s]	local speed of sound in jet medium
a_∞	[m/s]	speed of sound in acoustic room
$\boldsymbol{F}$	[-]	aerodynamic force (vector)
f	[Hz]	frequency
f_c	[Hz]	characteristic frequency
H	[m]	engine integration height
I	[W/m^2]	sound intensity
$\boldsymbol{I}$	[-]	identity matrix
L	[-]	engine integration length
L_0	[-]	characteristic length
M_{ac}	[-]	acoustic Mach number
M_c	[-]	convection Mach number
M_j	[-]	jet Mach number
$\boldsymbol{n}$	[-]	normal vector
p'	[Pa]	sound pressure
p_∞	[Pa]	(static) ambient pressure of acoustic room
r_U	[m]	velocity ratio between wind tunnel and jet velocity
r_0	[m]	distance source-observer
R_{mix}	[m]	mixed jet diameter
SPL	[dB]	sound pressure level
S	[-]	(surface) area
Sr	[-]	Strouhal number
$\boldsymbol{T}$	[Pa]	Lighthill's stress tensor
t	[s]	time
U_c	[m/s]	shear layer convection velocity
U_j	[m/s]	jet velocity
V	[m^3]	volume
v'	[m/s]	acoustic particle velocity
$\mathcal{F}$	[-]	dimensionless flight operations factor
$\mathcal{G}$	[-]	dimensionless geometry factor
$\mathcal{T}$	[-]	dimensionless temperature factor
$:$	[-]	double contraction

II. Analysing low-frequency JFI noise for compactness

For reason of consistancy, this section uses the notation and partial wording of a university lecture script (Delfs) for velocity scaling of compact noise in general. Yet, the approximations are adapted for the jet-flap interaction effect.

Fixed and rigid objects such as the wing and its flap generate excess noise due to the interaction of the body surface with unsteady flow fluctuations. The far-field solution has been derived by Curle[1] as well as Ffowcs-Williams and Hawkings[2] (see equation 1).

$$p' \simeq \underbrace{\frac{1}{4\pi a_\infty^2 r_0}(\boldsymbol{e}_{r_0}\boldsymbol{e}_{r_0}) : \frac{\partial^2}{\partial t^2}\int_{V'_\infty} \boldsymbol{T}\, dV}_{\text{(1) free turbulence}} + \underbrace{\frac{1}{4\pi a_\infty r_0}\boldsymbol{e}_{r_0} \cdot \frac{\partial}{\partial t}\int_{\partial V_B} (p\boldsymbol{I} - \boldsymbol{\tau}) \cdot \boldsymbol{n}\, dS}_{\text{(2) excess noise due to presence of object B}}. \tag{1}$$

Term (1) represents Lighthill's[3] solution for noise generated aerodynamically, which leads to the well-known result of free turbulence scaling with the eighth power of the characteristic velocity. Term (2) represents additional noise which is induced by the presence of the object. Especially the low-frequency part of the spectrum is of interest, which is called compact for frequencies lower than the characteristic frequency.

The characteristical distance L_0 is here defined as the difference between the engine integration length L and the virtual shear layer origin of the outer shear layer $x_{0,NF}$. The virtual shear layer origin can be determined by analysing the steady aerodynamic flow downstream the engine (Jente[4]) and is here located roughly at the midst of the pylon. The characterizing frequency f_c is calculated with $He = 1$ to $f_c = a_\infty / L_0$.

The integral in term (2) is interpreted as the net aero force on the body $\boldsymbol{F}$. The vector $\boldsymbol{e}_{r_0}$ accounts only for the net aero force component in the direction of the observer, therefore labeled as F_{r0}.

$$p'_{(2)} \simeq \frac{1}{4\pi a_\infty r_0}\frac{dF_{r0}}{dt} \tag{2}$$

The sound field is directly proportional to the time change of the net aero force on the body. Wrt jet-flap interaction, SenGupta[5] detected the same mechanism and called it lift fluctuation noise.

The magnitude of the aerodynamic force is estimated by the following jet parameters acting on a partial flap surface:

$$|\boldsymbol{F}| \propto \rho_{flap} U_{flap}^2 A_{flap} \tag{3}$$

Each parameter with index *flap* serves as a placeholder which should be proportional to some test parameter:

- We assume that only the outer part of the bypass jet shear layer is interacting with the flap ($H > R_{mix}$). Then, the velocity fluctuations may be assumed by the shear velocity ΔU.

  $$U_{flap}^2 \simeq (\Delta U)^2 \tag{4}$$

  Hypothetically, the velocity parameters in the thrust equation, $U_{flap}^2 \simeq U_j \Delta U$, could be a better scaling parameter, especially for radical engine integrations $H < R_{mix}$. This thought is challenged with experimental data (for builds with $H > R_{mix}$) in section III.

- The interaction area for $H > R_{mix}$ is very roughly approximated as half perimeter of the jet ("along flap span") and shear layer width ("along flap chord") δ_ω. The shear layer width (and hence the relevant interaction area) changes wrt velocity according to thin mixing layer theory (e.g. Eisfeld[6] by $\delta_\omega \propto L_0 \Delta U / U_c$

  $$A_{flap} \propto \pi R_{mix} \delta_\omega \tag{5}$$
  $$A_{flap} \propto \pi R_{mix} L_0 \Delta U / U_c \tag{6}$$

  This approximation does only poorly state the dependencies of other geometric properties which have a clear influence. Yet, the formulation is sufficient for the purpose of this paper and may be expanded to include build sensitivities.

- In order to account for differences in static temperature between jet stream and flight stream, the density term is approximated as a mix between the two streams:

  $$\rho_{flap} = \sqrt{\rho_j \rho_\infty} \tag{7}$$

  For the purpose of this paper, the exact estimation is not important (there is only cold test data with too small temperature differences to prove or disprove the proper temperature dependency). Alternatives are (A) $\rho_{flap} = \rho_\infty$, argueable if the flap trailing edge is far away from the jet and (B) $\rho_{flap} = \rho_j$ if the (core) jet is very close to the trailing edge.

All in all, the magnitude of the force is estimated as

$$|\boldsymbol{F}| \propto \sqrt{\rho_j \rho_\infty} \frac{(\Delta U)^3}{U_c} \pi R_{mix} L_0 \tag{8}$$

The time change of the force occurs during the characteristic period t_c it takes to convect a flow disturbance along the wing, i.e. $t_c \propto L_0/U_c$. This relation is used to approximate the time derivative $\frac{\partial}{\partial t} \propto 1/t_c = U_c/L_0$.

The sound intensity of a compact body scales like

$$I = \overline{p' v'_{r0}} \simeq \frac{\overline{p'^2}}{\rho_\infty a_\infty} \tag{9}$$

$$\boxed{I \propto \frac{{R_{mix}}^2}{r_0^2} \frac{\rho_j}{a_\infty^3} (\Delta U)^6} \tag{10}$$

The sound intensity of the compact JFI noise for non-radical engine integrations scales with the sixth power of the difference velocity ΔU.

For purpose of analysis, it is helpful to decompose sound intensity into the following factors: Flight operations effect $\mathcal{F}$, Temperature effect $\mathcal{T}$ and Geometry $\mathcal{G}$. This is done by using the relations $\rho_j = \gamma_j p_\infty / a_j^2$ (i.e. ideal gas and definition of speed of sound) as well as $\Delta U = U_j(1 - r_U)$ with the velocity ratio between the flight velocity and the jet velocity $r_U = U_\infty / U_j$:

$$I \propto p_\infty \frac{{R_{mix}}^2}{r_0^2} \frac{\gamma_j}{a_j^2 a_\infty^3} U_j^6 (1 - r_U)^6 \tag{11}$$

$$\tag{12}$$

Furthermore, the aerodynamic jet Mach number $M_j = U_j/a_j$ as well as the acoustic Mach number $M_{ac} = U_j/a_\infty$ are introduced (same procedure as by Jente[7]).

$$I \propto p_\infty U_j \underbrace{\gamma_j M_j^2 M_{ac}^3}_{\mathcal{T}} \underbrace{(1 - r_U)^6}_{\mathcal{F}} \underbrace{\frac{{R_{mix}}^2}{r_0^2}}_{\mathcal{G}} \tag{13}$$

This results in equation 13 where sound intensity is displayed by pressure $\times$ velocity and otherwise the following non-dimensional terms:

- Geometry term $\mathcal{G}$ is here roughly estimated and may be expanded for build changes. It features the typical exponent of 2 for sound intensity.
- The flight operations term $\mathcal{F}$ depends on the velocity ratio $r_U = U_\infty/U_j$ and converges to a constant for same velocity ratio. This does especially include static jets, i.e. $r_U = 0$. The term has been derived for $H > R_{mix}$. This function may change depending on H (see equation 4). Radically integrated installations $H < R_{mix}$ might scale with a lower exponent, i.e. $(1 - r_U)^4$.

$$\mathcal{F} = \begin{cases} (1 - r_U)^6 & U_{flap}(H > R_{mix}) = \Delta U \\ (1 - r_U)^4 & U_{flap}^2(H < R_{mix}) = U_j \Delta U \end{cases} \tag{14}$$

- The temperature term $\mathcal{T}$ term postulates that same static Mach numbers (at different temperatures) should lower the velocity scaling exponent from 6 to 4. It is very important to study the role of any hot core stream jet, since cold tests show that the core jet deflects from the core engine axis to into flap direction in order to fill up the wake area just behind the pylon.

$$\mathcal{T} = \begin{cases} \gamma_\infty M_{ac}^5 & \rho_{flap}(H \gg R_{mix}) = \rho_\infty \\ \gamma_j M_j^2 M_{ac}^3 & \rho_{flap}(H > R_{mix}) = \sqrt{\rho_j \rho_\infty} \\ \frac{\gamma_j^2}{\gamma_\infty} M_j^4 M_{ac} & \rho_{flap}(H < R_{mix}) = \rho_j \end{cases} \tag{15}$$

This paper deals with cold test data only. Hence, the temperature dependence cannot be tested well.

III. Experiment

Experimental data was generated at the Aeroacoustic Wind tunnel Braunschweig[8] (AWB), a DLR test facility in Northern Germany. A SAFRAN UHBR short cowl dual stream engine model was integrated onto the AIRBUS RDJ80 wing and connected via pylon.

This section should also list characteristic build properties, i.a. mixed jet radius/diameter, engine integration length and height, as well as virtual shear layer origin in the final version. Operational parameters of the test campaign are defined by wind tunnel velocity U_∞ and jet velocity U_j and displayed in figure 1.

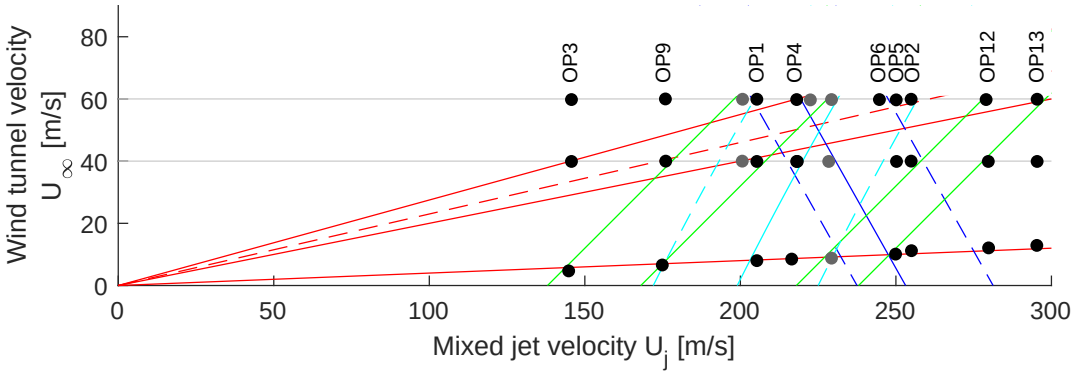

Figure 1: Wind tunnel test operations with iso-contours of constant velocity ratio r_U (red), shear layer difference velocity ΔU (green), shear layer convection velocity U_c (blue) and idealized thrust (cyan).

Finding the velocity scaling of JFI noise is an iterative process which consists of formulating a test hypothesis (here based on the analytical derivation in section II) and challenging the hypothesis against experimental data.

The derivation process in section II produces the following velocity candidates:

- shear layer difference velocity $\Delta U = U_j(1 - r_U)$
- shear layer convection velocity $U_c = U_j(r_U + \alpha(1 - r_U))$, with $\alpha = 0.64$.
- operations which produce approximately the same thrust can be detected by calculating $U_{th} = U_j\sqrt{1 - r_U}$

In order to force a smart observer position, one velocity candidate is kept constant at a time while other velocity candidates and scaling exponents are varied. The uncertainty and quality of the found scaling exponent depends on the gain difference ΔSPL_0 of the unscaled data.

1. The process starts with finding the combined velocity scaling exponent by cross-comparing the **same velocity ratio operations**, i.e. $r_U = \text{const}$. Since these velocity profiles are self-similar, it does not matter which velocity candidate is used for scaling, all parameters have the same proportionality to each other. This includes the set of the tested quasi-static conditions ($r_U \approx 0.04$, see figure 2): The low-frequency noise $He < 1$ scales with a velocity exponent close to $q = 6$. The high-frequency spectrum scales with exponent $q = 8$, which is the expected result for free turbulence (term (1) in equation 1).

2. Then, operations with **constant shear layer convection velocity** are chosen. A special feature of these operations is that the same convection velocity results in the same Doppler terms for each microphone, or in other words: fully comparable directivity.

   Note, that the relevant flap surface area depends on velocity components (equation 6). If this surface area was assumed invariant to velocities instead, the sound intensity would be proportional to $U_c^2(\Delta U)^4$. This is why $q = 4$ is checked, as well as $q = 5$ (trailing edge noise) and $q = 6$ (compact noise, as derived in equation 10).

   The scaling for $U_c = 180\text{m/s}$ (see figure 4) collapses well for $(\Delta U)^6$. Note that does not only affect low-frequency noise, but the entire spectrum. This is no accident, since jet shear layer noise has been reported to scale as $I \propto U_c^2(\Delta U)^6$. (see Jente[9] for low r_U or Michalke/Michel,[10] equation 4.31 for $A = 2$).

Note, how similar the shape functions are. One might come up with the idea to identify shape functions for all U_c and use them for modelling the JFI effect. However, it must be admitted, that the operations are not too different (scaling difference is only 3dB, not 10dB). Hence, more than one U_c has to be checked for its shape.

3. The ultimate prove for dependence on ΔU alone is testing operations with **same shear layer difference velocity**. According to equation 10, these profiles should collapse by default and show a gain difference close to zero. This test alone does not give

4. In order to remove any doubt on the approximation of the relevant flap velocity in equation 4, checks can be made to rule out the thrust option $|\boldsymbol{F}| \propto U_j \Delta U$, e.g. by using **same jet velocity** operations. There is another advantage of this test compared to 2.: The gain difference of the data to be scaled is very large. Hence, there is greater certainty in the determined scaling exponent.

   The exponent $q = 4$ supports the jet thrust approximation, $q = 6$ the compact noise derivation and $q = 5$ trailing edge noise.

   According to the results in figure 6 for $q = 4$, the dependency on thrust can be ruled out. Moreover, $q = 5 \ldots 6$ scales very nicely for the high frequencies, since the conditions are jet-noise like (compare Michalke/Michel,[10] equation 4.31 for $A = 1$). However, the shape functions for $He < 1$ vary and look better for same shear layer convection velocity (figure 4).

5. With the same reason as in 4., operations with **same wind tunnel velocity** U_∞ can be checked. There is also the advantage of large gain difference ($8 - 9$dB).

   The low-frequency scaling looks promising for both $q = 5$ and $q = 6$ (see figure 7)

The following figures 2 to 7 show third-octave sound pressure level as gain. The narrowband data is deformed (see Gaeta/Ahuja[11]) in order to match the shape of the third octave spectrum. The right diagram features the scaling of two or three velocity exponents q. In order to fit the scalings for each q canditate in one diagram, the reference velocity U_{ref} depends on q to create a 12 dB difference.

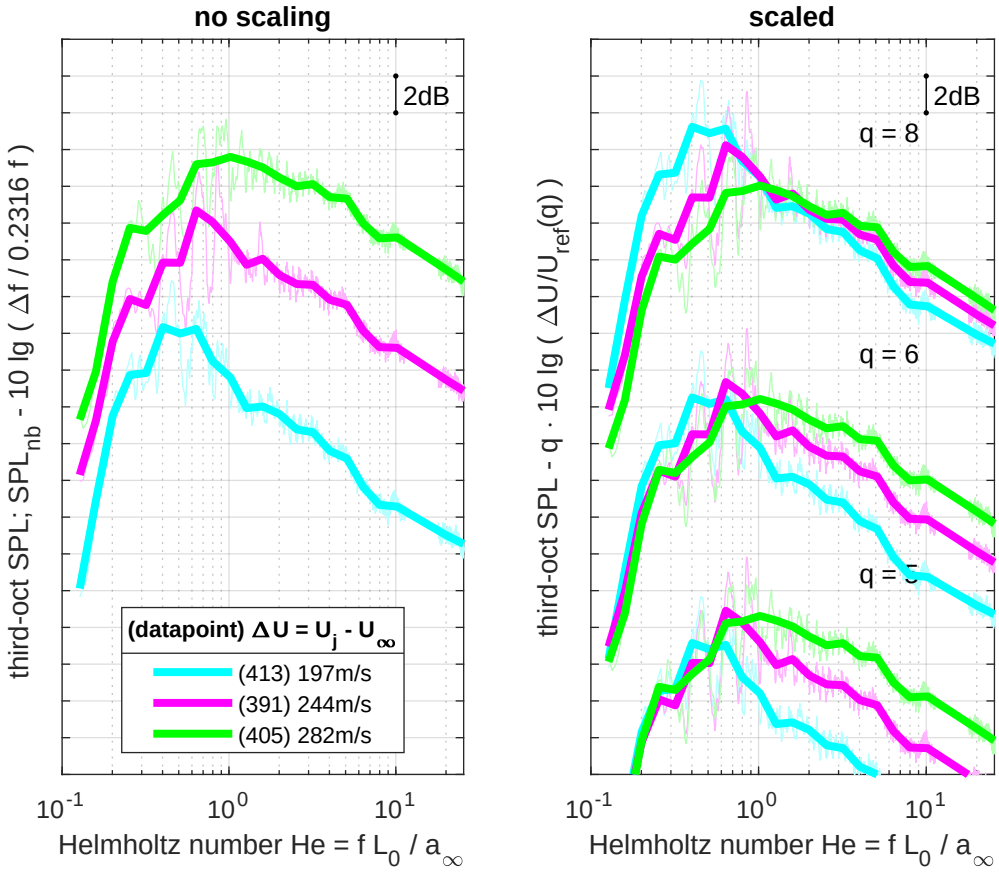

Figure 2: Same velocity ratio $r_U = 0.04$ (quasi-static jet)

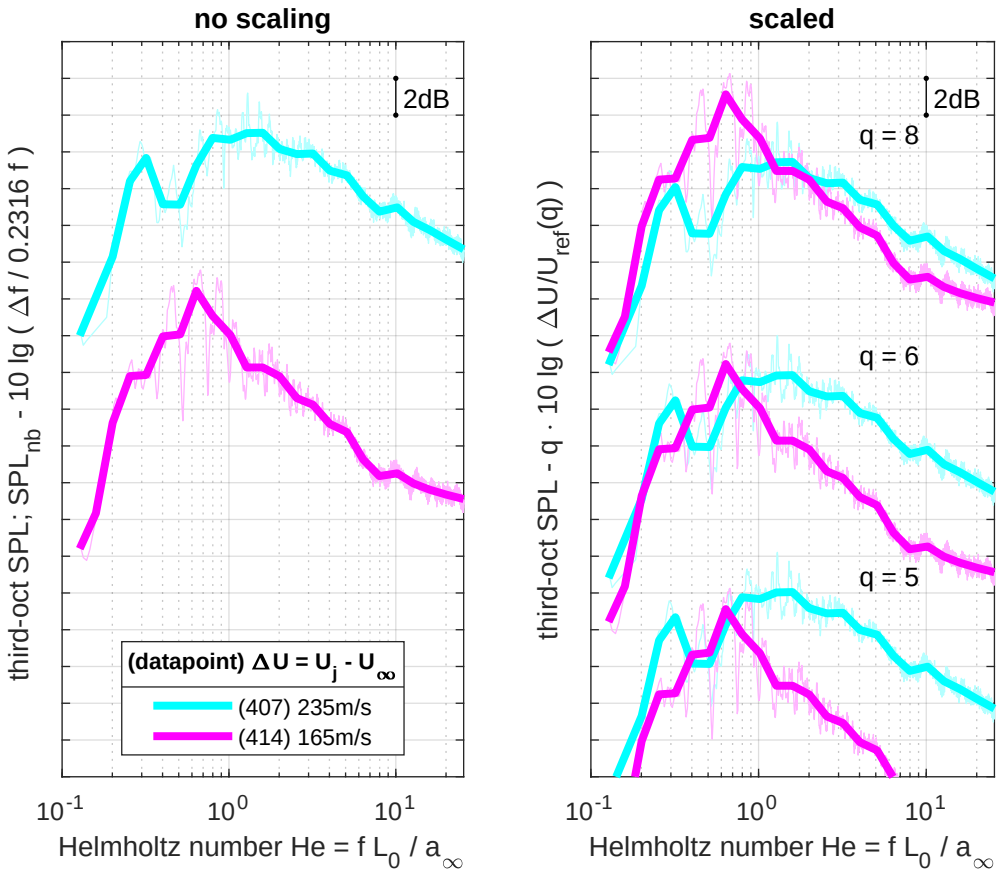

Figure 3: Same velocity ratio $r_U = 0.20$

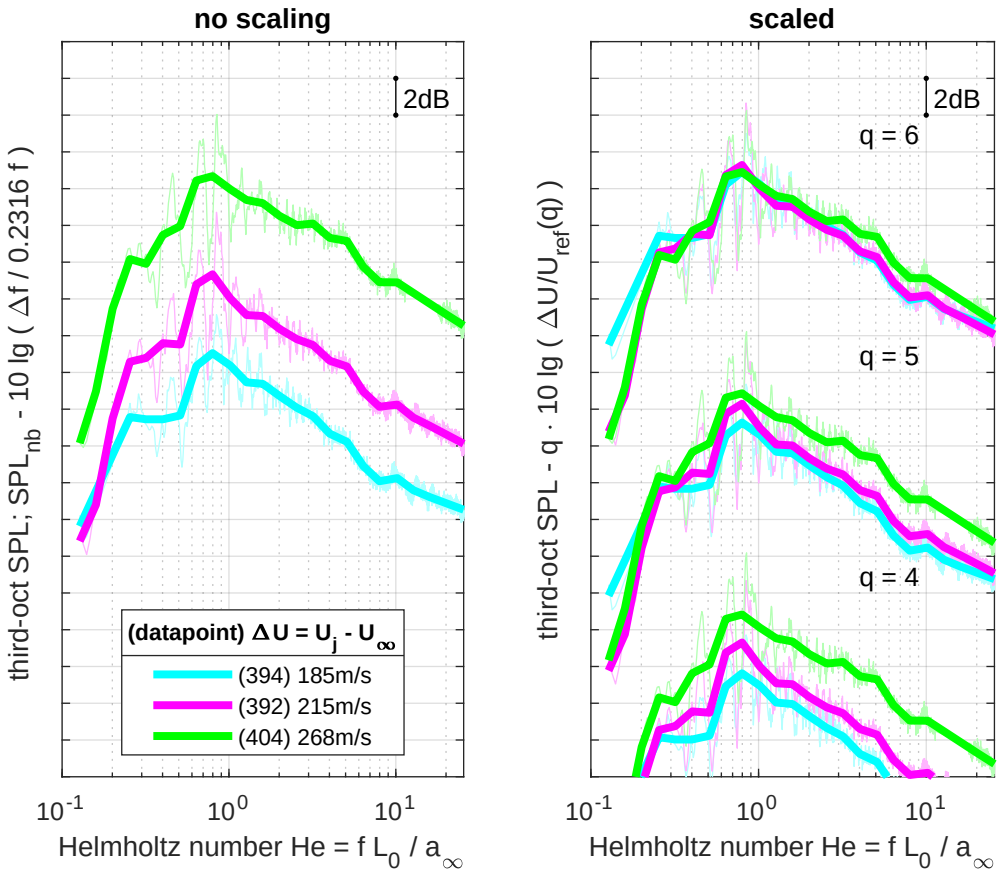

Figure 4: Same shear layer convection velocity $U_c = 180\text{m/s}$

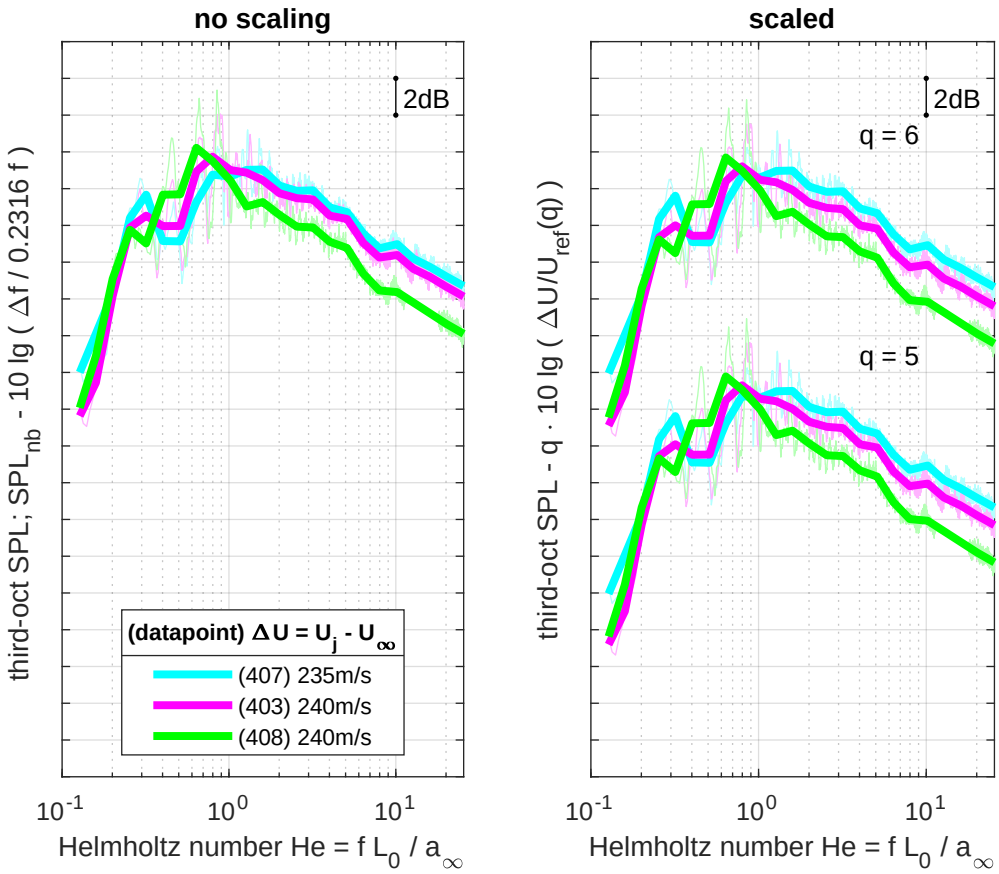

Figure 5: Same shear layer difference velocity $\Delta U \approx 235\text{m/s}$

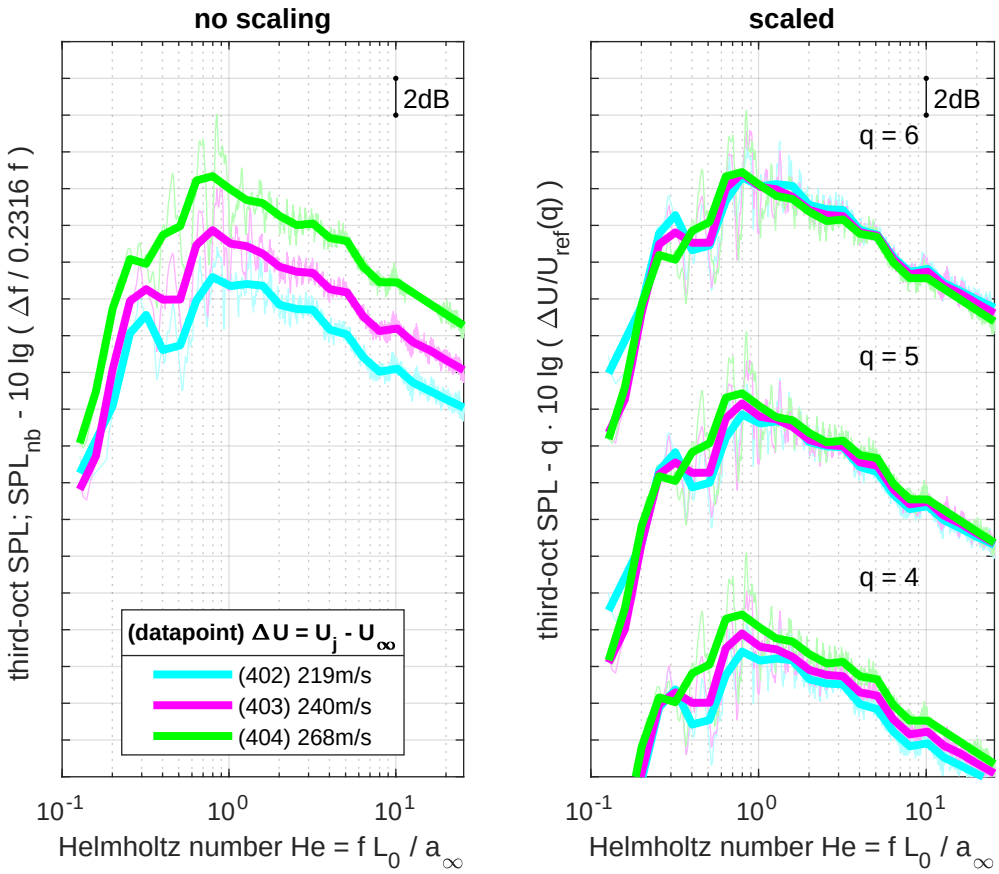

Figure 6: Same jet velocity $U_j \approx 280\text{m/s}$

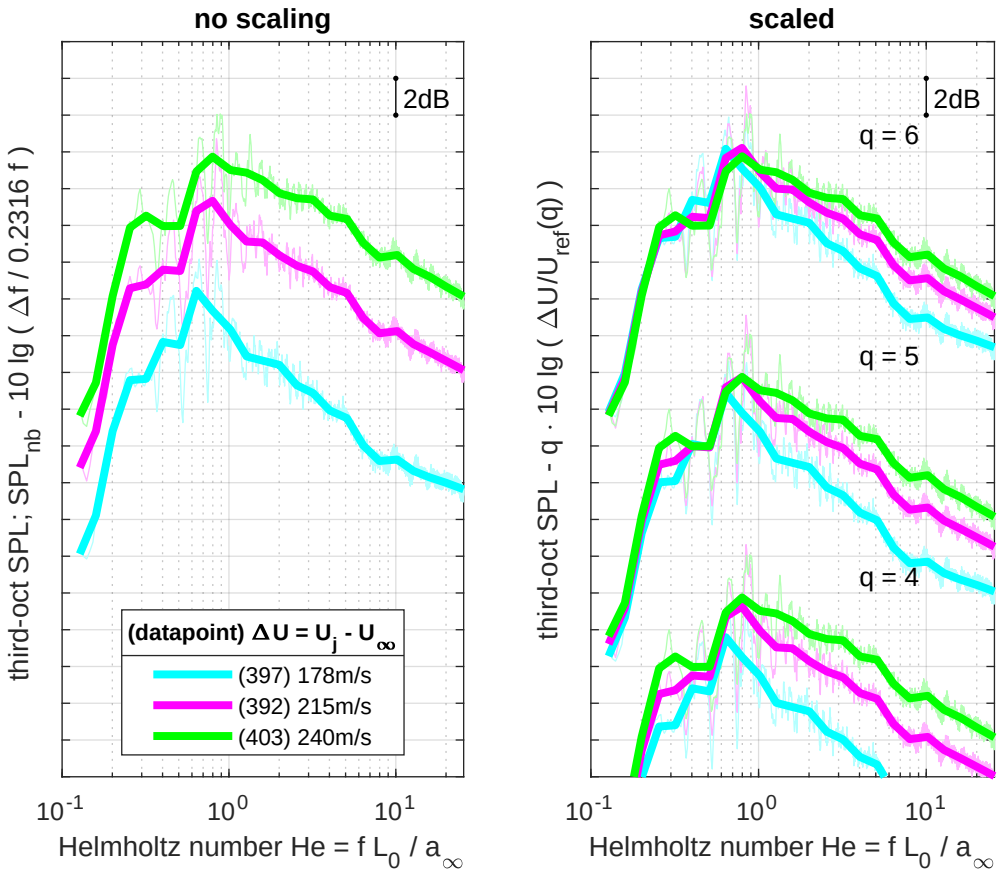

Figure 7: Same wind tunnel velocity $U_\infty = 40\text{m/s}$

IV. Conclusion

This paper confirms the validity of the Curle and FWH terms for JFI noise of a pylon-mounted engine. The far-field sound intensity of the compact low-frequency noise $He < 1$ is proportional to $I \propto (\Delta U)^6$. This has been derived and experimentally checked for engine integrations $H > R_{mix}$. The high-frequency part of the spectrum collapses well for $I \propto U_c^2(\Delta U)^6$.

It was discovered that the full spectrum collapses neatly with $(\Delta U)^6$, if operations with same shear layer convection velocity U_c are chosen. This implies that for a semi-emperical JFI noise model, shape functions for a number of different convection velocities should be derived. In theory, this is possible using only static JFI test data, e.g. from a static jet test facility.

Acknowledgments

The EU DJINN (Decrease Jet Installation Noise) project receives funding from the European Union's Horizon 2020 research and innovation programme under grant agreement No 861438. DJINN is a collaborative effort between CFD-Berlin (coordinator), Airbus SAS, Dassault Aviation, Safran Aircraft Engines, Rolls-Royce Deutschland, ONERA, DLR, University of Southampton, CERFACS, Imperial College London, von Karman Institute, CNRS, and Queen Mary University of London.

References

[1]Curle, N. and Lighthill, M. J., "The influence of solid boundaries upon aerodynamic sound," *Proceedings of the Royal Society of London. Series A. Mathematical and Physical Sciences*, Vol. 231, No. 1187, 1955, pp. 505–514.

[2]Ffowcs Williams, J. E., Hawkings, D. L., and Lighthill, M. J., "Sound generation by turbulence and surfaces in arbitrary motion," *Philosophical Transactions of the Royal Society of London. Series A, Mathematical and Physical Sciences*, Vol. 264, No. 1151, 1969, pp. 321–342.

[3]Lighthill, M. J., "On sound generated aerodynamically I. General theory," *Proceedings of the Royal Society of London. Series A. Mathematical and Physical Sciences*, Vol. 211, No. 1107, 1952, pp. 564–587.

[4]Jente, C., "Steady aerodynamics flow analysis for determining the necessary build space of an isolated jet shear layer," *EU H2020 1st DJINN Conference: Industrially oriented jet noise reduction technologies*, Dezember 2021.

[5]SENGUPTA, G., "Analysis of jet-airframe interaction noise," *8th Aeroacoustics Conference*, Aeroacoustics Conferences, American Institute of Aeronautics and Astronautics, 1983.

[6]Eisfeld, B., "Reynolds Stress Anisotropy in Self-Preserving Turbulent Shear Flows," Tech. rep., DLR, Juni 2017.

[7]Jente, C., "Acoustic Mach number, jet Mach number or jet velocity: Choosing the optimal control property for jet noise experiments at different test rigs," *28th AIAA/CEAS Aeroacoustics Conference, 2022*, Juni 2022, pp. 1–13.

[8]Pott-Pollenske, M. and Delfs, J., "Enhanced Capabilities of the Aeroacoustic Wind Tunnel Braunschweig," *14th AIAA/CEAS Aeroacoustics Conference (29th AIAA Aeroacoustics Conference)*, American Institute of Aeronautics and Astronautics.

[9]Jente, C. and Delfs, J., "Velocity Scaling of Shear Layer Noise induced by cold Jet flow with co-flowing Flight stream," *25th AIAA/CEAS Aeroacoustics Conference*, Aeroacoustics Conferences, American Institute of Aeronautics and Astronautics, 2019.

[10]Michalke, A. and Michel, U., "Prediction of jet noise in flight from static tests," *Journal of Sound and Vibration*, Vol. 67, No. 3, 1979, pp. 341–367.

[11]Gaeta, R. and Ahuja, K., "Subtle Differences in Jet Noise Scaling with Narrow Band Spectra Compared to 1/3-Octave Band," *9th AIAA/CEAS Aeroacoustics Conference and Exhibit*, Aeroacoustics Conferences, American Institute of Aeronautics and Astronautics, 2003.